



## RESEARCH ARTICLE

**Dielectric relaxation, AC conductivity and photoluminescence properties of poly (p-phenylenediamine)/TiO<sub>2</sub>nanocomposites**

Archana S and Jaya Shanthi R\*

Department of Chemistry, Auxilium College, Vellore-632006, Tamil Nadu, India.

**Manuscript Info****Manuscript History:**

Received: 25 August 2014  
Final Accepted: 22 September 2014  
Published Online: October 2014

**Key words:**

polyphenylenediamine,  
nanocomposite, thermal property,  
photoluminescence

**\*Corresponding Author****Archana S****Abstract**

Poly (p-phenylenediamine) and their nanocomposites with TiO<sub>2</sub> nanoparticles were prepared and characterized using spectral techniques like FT-IR, UV-VIS spectroscopy and the morphology have been studied by XRD, SEM and TEM. The stability of the prepared polymer nanocomposites was analyzed using TGA, DTA and found to have high thermal stability. The study of dielectric and photoluminescence property was studied. The results showed these materials can be used as semiconductor and diodes.

*Copy Right, IJAR, 2014,. All rights reserved***Introduction**

Nanocomposites constitute a new class of material that involves nano-scale dispersion in a matrix. Nanocomposites have at least one ultrafine phase dimension, typically in the range of 1-100nm and exhibit improved properties when compared to micro- and macro-composites (Paulo Meneghetti et al., 2006). Nanocomposites formed by immobilization of metal nanoparticles into the conjugated conducting polymer matrices, such as polypyrrole, polyaniline, or polythiophene, have received much attention in recent days because of their potential use in various fields (Paulraj et al., 2011). Incorporation of nanostructured inorganic compounds into the polymer will facilitate the combination of different features of organic and inorganic species, and the inorganic fillers in the nano form are expected to modify the properties of the conducting polymers leading to the development of multifunctional devices. The inorganic fillers at nanoscale exhibit high surface to volume ratio and thus expected to modify drastically the electrical, optical, and dielectric properties of polymer (Jalal Arjomandi et al., 2014). Among the conducting polymers, poly(phenylenediamine), a highly aromatic polymer containing 2,3-diaminophenazine or quinoraline repeating unit has received significant attention because it can be utilized in many fields (Muthirulan et al., 2013), (Mei-Rong et al., 2001). Among all the nanoparticles TiO<sub>2</sub> has the merits of low cost, structural stability, non-toxicity, large energy gap, dielectric constant, and environmental-friendliness and easy to synthesis (SubodhSrivastava et al., 2011).

Mona H. Abdel Rehim et al synthesized poly (phenylenediamine) with TiO<sub>2</sub> nanocomposite which act as hydrogen storage material (Mona et al., 2011). PandiMuthirulan et al., (PandiMuthirulan et al., 2013) and Hui-Long Wang et al.,(Hui-Long Wang et al., 2012) have successively prepared the nanocomposites of PpPDA with TiO<sub>2</sub> to enhance the photocatalytic activity and the photocatalytic degradation of Rhodamine B and methylene blue. Pengwei Huo et al prepared poly (o-phenylenediamine)/TiO<sub>2</sub>/fly-ash cenospheres and its photo-degradation property on antibiotics under visible light irradiation (PengweiHuo et al., 2010).

The PoPDA-MnO<sub>2</sub> nanocomposite was prepared to enhance the specific capacitance of polymer. Meirong Wang et al prepared the PoPDA-MnO<sub>2</sub> nanocomposites and they applied the formed nanocomposites in the field of supercapacitors (Meirong Wang et al., 2013).

In the present study the conducting Poly (p-phenylenediamine) (PpPDA) has been prepared via chemical oxidative polymerization method. The nanocomposites of PpPDA with TiO<sub>2</sub> nanoparticles with different weight percentage of 10, 20 and 30 wt % were prepared and their photoluminescence (PL) and dielectric property were studied. This study is the first attempt to use PpPDA nanocomposites to study the PL and dielectric properties.

## 2. Materials and Methods

### 2.1 Materials

The monomer p-phenylenediamine, ferric chloride, surfactant Sodium Dodecyl Sulfate was purchased from Merck, all the other chemicals and reagents were of Analytical Grade and used as received without further purification. The nanoparticles of TiO<sub>2</sub> were purchased from Sigma Aldrich of particle size 50-55nm.

### 2.2 Methods

#### Synthesis of poly (p-phenylenediamine) with TiO<sub>2</sub> nanoparticles

The equimolar volume of p-phenylenediamine and hydrochloric acid was prepared and TiO<sub>2</sub> is added in the weight percentages of 10, 20 and 30% to the above solution and kept for vigorous stirring to keep the TiO<sub>2</sub> suspended in the solution. To this, SDS was added as an emulsifier and ferric chloride was added drop wise as an oxidant. The obtained solutions were kept for stirring at room temperature for 6 h to polymerize the monomers. The poly (p- phenylenediamine) -TiO<sub>2</sub> nanocomposites (PpPDA/TiO<sub>2</sub>) precipitate was collected on filtration, washed with deionised water followed by methanol to remove the oligomers and unreacted monomers present in the polymers (Aashish Roy et al., 2013).

#### 2.3 Characterization techniques

The FT-IR of the synthesized samples was recorded on an ABB-MB-3000 FT-IR spectrometer in KBr medium. The UV-Vis spectrum of polymers was taken using Perkin Elmer Lambda UV-Vis- Spectrometer by dissolving the polymers in DMSO as a solvent. The XRD was measured with Bruker AXS D8 Advance using Cu as X-ray source at the Wavelength of 1.5406 Å of angular range from 3° to 135°. Scanning electron microscopy was used to study the morphology of the synthesized polymers using JEOL, JSM-6390LV model. High-resolution transmission electron microscopy was measured using Tecnai T20 G2 S-TWIN of operating voltage 250 kV. TG/DTA was recorded using Perkin Elmer STA 6000 model. Fluorescence was measured using the instrument spectrofluorometer of model FLUOROLOG-FL3-11. The Broadband Dielectric Spectrometer (BDS) was measured in pellet form using NOVOCONTROL Technologies, GmbH & Co. Germany, Concept 80 model. Differential Scanning Calorimetry (DSC) was measured using Mettler Toledo DSC 822e from room temperature to 300°C.

## 3. Results and discussion

### 3.1 FT-IR spectroscopy

The FT-IR spectrum of the PpPDA prepared with 10% of TiO<sub>2</sub> (PpPDA/10%TiO<sub>2</sub>), 20% of TiO<sub>2</sub> (PpPDA/20%TiO<sub>2</sub>) and 30% of TiO<sub>2</sub> (PpPDA/30%TiO<sub>2</sub>) are given in Fig. 1. From the figure it is evident that a single band at 3225 cm<sup>-1</sup> is due to N-H stretching vibrations of the -NH-group. The two peaks at 3337, 2950 cm<sup>-1</sup> are ascribed to the asymmetrical and symmetrical of N-H stretching vibrations of NH<sub>2</sub> group. Two strong peaks at 1590 cm<sup>-1</sup> and 1502 cm<sup>-1</sup> are associated with the stretching vibrations of C=N and C=C group in phenazine ring. The peaks at 1396 cm<sup>-1</sup> and 1240 cm<sup>-1</sup> are associated with C-N-C stretching in the benzenoid and quinoid imine units. The peaks at 830 cm<sup>-1</sup> and 572 cm<sup>-1</sup> can be attributed to the out-of-plane deformation of C-H on a 1, 2, 4- tetra substituted benzene ring, which implied that the polymers had the basic phenazine skeleton (Siwei Yang et al., 2012), (Xiaofeng Lu et al., 2007). It can be also noticed from figure that the characteristic bands of PpPDA are shifted toward lower wavenumber indicating that there is strong interaction between TiO<sub>2</sub> and the polymer chains (Mona et al., 2011). The shift in the peaks of the polymer nanocomposites is due to formation of hydrogen bonding between oxygen of TiO<sub>2</sub> with hydrogen of -NH- group present in the polymer (Rajeev sehwat 2009). In addition to the above peaks, the presence of peak at 454 cm<sup>-1</sup> confirms M-O bond stretching vibration of TiO<sub>2</sub> and this confirms the incorporation of TiO<sub>2</sub> into the polymeric matrix. The S=O peak at 1152 cm<sup>-1</sup> confirms that the emulsifier SDS is also incorporated into the polymeric backbone.

### 3.2 UV-Vis spectroscopy

The UV-Vis spectrum of PpPDA/10%, PpPDA20% and PpPDA30% of TiO<sub>2</sub> are given in Fig.2 and it shows major peaks around 300 nm and 460 nm. The band around 460 nm is assigned to π-π\* transition associated with the phenazine ring conjugated to the two lone pair of electrons present on the nitrogen of the NH<sub>2</sub> groups. The

peaks are broad and it suggests the existence of quinoneimine moieties. The other peaks around 300 nm is due to  $\pi$ - $\pi^*$  transitions of the benzenoid and quinoid structures (Liang Wang et al., 2008).

### 3.3 X-ray power diffractometer

The XRD spectrum of PpPDA/TiO<sub>2</sub> with 10, 20 and 30 wt% was given in the Fig.3. For TiO<sub>2</sub>, the peaks at  $2\theta = 25.38, 37.88, 48.08, 53.98$  and  $55.18$  can be assigned to the diffractions of the (1 0 1), (0 0 4), (2 0 0), (1 0 5), and (2 1 1) crystal planes of anatase phase. The characteristic diffraction peaks observed at  $27.48$  and  $36.18$  can be attributed to the (1 1 0) and (1 0 1) faces of rutile phase in TiO<sub>2</sub> (Deivanayaki et al., 2012).

The XRD patterns of PpPDA/TiO<sub>2</sub> composites show the characteristic peaks not only for the PpPDA which is  $5^\circ < 2\theta < 35^\circ$  but also for the TiO<sub>2</sub> nanoparticles, proving the existence of TiO<sub>2</sub> nanoparticles within the composite. This confirms that the PpPDA/TiO<sub>2</sub> nanocomposites become more crystalline as the concentration of TiO<sub>2</sub> is increased. The PpPDA deposited on the surface of TiO<sub>2</sub> particles has not affected the crystallization behavior of TiO<sub>2</sub> particles in the nanocomposites (SubodhSrivastava et al., 2011).

### 3.4 Scanning electron microscopy

The morphology of the PpPDA with 10, 20 and 30% TiO<sub>2</sub> was found using scanning electron microscopy and their images are given in Fig. 4a-c. The figure shows a porous and irregular structure. There is large number of clews present in the polymer. The irregular shapes and the porous nature of the compacted powders are evidenced by the images taken at high magnification (Elasayed et al., 2011). The surfaces of the polymer are having highly agglomerated grains due to TiO<sub>2</sub> nanoparticles dispersed evenly into polymer matrix and this may change the properties of PpPDA. The formation of grains was found to be increase with the increase in the TiO<sub>2</sub> nanoparticles. From the image it is evident that the PpPDA/TiO<sub>2</sub> nanocomposites are having the properties of both PpPDA and TiO<sub>2</sub> nanoparticles.

### 3.5 Transmission Electron Microscopy

HRTEM was used to image the PpPDA with 30%TiO<sub>2</sub> and the HRTEM image of PpPDA/30%TiO<sub>2</sub> is found to have aggregated spherical like morphology. From the Fig. 5a-c it is evident that the entire surface of the TiO<sub>2</sub> particles are surrounded by PpPDA in a uniform manner and the TiO<sub>2</sub> nanoparticles are well dispersed in the polymer matrix. Moreover, the outer shell of the particle exhibited a fine increment in brightness compared with the dark inner core and this confirms the formation of core-shell feature of the PpPDA/TiO<sub>2</sub> nanocomposites. The formation of PpPDA encapsulated TiO<sub>2</sub> core-shell nanocomposites was attributed to the strong electrostatic interaction between PpPDA and TiO<sub>2</sub> (Deivanayaki et al., 2012). The particles size of the synthesized polymer nanocomposites falls in the range of 50-60nm.

### 3.6 Thermo Gravimetric / Differential Thermal Analysis

The TGA of PpPDA at different concentrations of TiO<sub>2</sub> nanoparticles like 10%, 20% and 30% are found to have three stages of thermal transition (Fig. 6). The first thermal transition from 180 to 280°C is ascribed to the removal of dopants molecules. The second thermal transition from 310 to 480 °C are corresponds to the loss of low molecular weight oligomers or side products present in the polymer nanocomposites. The third transition starts from 500°C and continues up to 732 °C with a weight loss of ~30% and this can be attributed to the degradation of benzenoid and quinonoid repeating units of the polymeric backbone (Muthirulan et al., 2012). The residue left at the end of the heating process is found to be 2.6376 mg for PpPDA/10% TiO<sub>2</sub>, 3.5807 mg for PpPDA/20%TiO<sub>2</sub> and 4.105 mg for PpPDA/30%TiO<sub>2</sub>. The amount of residue is found to increase with the increase in the percentage of TiO<sub>2</sub> nanoparticles and this confirms the incorporation of metal oxide into the polymer.

DTA curves of PpPDA/10%, 20% and 30% TiO<sub>2</sub> shows a wide peak with a plateau in temperature range of 400–705°C and this is related to the decomposition of organic moiety. The peaks related to the main stage of decomposition of the polymer are shown in Fig. 7. The TGA and DTA study confirms that the synthesized polymer nanocomposites possess good thermal stability.

### 3.7 Differential Scanning Calorimetry

DSC can be used to obtain the thermal critical points like melting point (T<sub>m</sub>), enthalpy specific heat or glass transition temperature (T<sub>g</sub>) of substances. The DSC spectrum of PpPDA/30%TiO<sub>2</sub> is given in Fig.8 and it shows an endothermic peak at 96.28°C which is due to the glass transition temperature. The polymer starts to melt above 260°C which are shown by endothermic peak at 274.62°C which is characteristics of melting temperature (Alan Riga et al., 1988).

### 3.8 Photoluminescence property

Photoluminescence (PL) is the property which involves the process of photon excitation followed by photon emission. At room temperature most molecules occupy the lowest vibrational level of the ground electronic state, and on absorption of light, they are elevated to produce excited states. From there the molecules again lose energy until the lowest vibrational level of the first excited state. From this level, the molecule can return to any of the vibrational levels of the ground state, emitting its energy in the form of fluorescence [Perkin Elmer, 2000]. The PL spectrum of polymers and their nanocomposites were recorded and are shown in the Fig. 9. The PpPDA prepared

with 10, 20 and 30% TiO<sub>2</sub> are found to fall under the green light emission region with the intensity of 4,85,875 for PpPDA/10% TiO<sub>2</sub>, 5,78,671 for PpPDA/20% TiO<sub>2</sub> and 7,54,811 for PpPDA/30% TiO<sub>2</sub>. Thus the polymer and there nanocomposites are found to have green light emitting property. The result also confirms that the presence of TiO<sub>2</sub> nanoparticles increases the PL properties PpPDA upon incorporation into polymer matrix. Thus the synthesized nanocomposites can be used as a green light emitter.

### 3.9 Dielectric Analysis

The real part of complex permittivity  $\epsilon'$  (dielectric permittivity) indicates the ability of the material to store energy from the applied electrical field. The imaginary part of complex permittivity  $\epsilon''$  (dielectric loss factor) is the dielectric loss factor or the dissipation factor represents the energy loss from the absorption process, and is a ratio of the energy which is dissipated to the energy stored in the material (Matthew et al., 2008). The plot of  $\epsilon'$  and  $\epsilon''$  against frequency for the PpPDA with TiO<sub>2</sub> nanocomposites prepared with 10, 20 and 30 wt% was given in the Fig. 10 and 11 respectively. From the figure it was found that the both  $\epsilon'$  and  $\epsilon''$  were found to increase with the decrease of frequency below 2Hz for all the synthesized polymer nanocomposites. The increment in  $\epsilon'$  with decrease in frequency reveals that the systems exhibit strong interfacial polarization at low frequency. The dielectric permittivity is found to increase with the increase in percentage of TiO<sub>2</sub> nanoparticles. The PpPDA/30%TiO<sub>2</sub> have high dielectric constant compare to the other nanocomposites and this may be due to the dielectric relaxation i.e., because of the movement of dipole and charge carriers due to the applied alternating field (Ramesh Patil et al., 2012).

To maximize efficiency and prevent problems such as dielectric heating (high-power) or signal loss (low-power), it is usually desirable to have a material with a low dissipation factor. The dielectric loss decreases with increase in frequency for all the polymer and nanocomposites. The polymer nanocomposites are having low dielectric loss when compare to the polymers. Among them PpPDA/30%TiO<sub>2</sub> has low dielectric loss when compare to other synthesized materials. The low frequency dispersion for  $\epsilon'$  and no loss peak for  $\epsilon''$  are characteristics of charged carrier systems (Bluma et al., 2006).

The plot of tangent loss against ( $\tan \delta$ ) frequency is given in Fig. 12. The high  $\tan \delta$  dissipation loss at low frequency in the polymer may be due to DC conduction losses. At low frequencies, the dielectric loss is found to increase and then decreases for polymer. Peak appearing at a characteristic frequency suggest the presence of relaxing dipoles in the samples. At higher frequencies the nanocomposites exhibits almost zero dielectric loss which suggests that these polymers are lossless materials at frequencies beyond a certain frequency (Machappa et al., 2009).

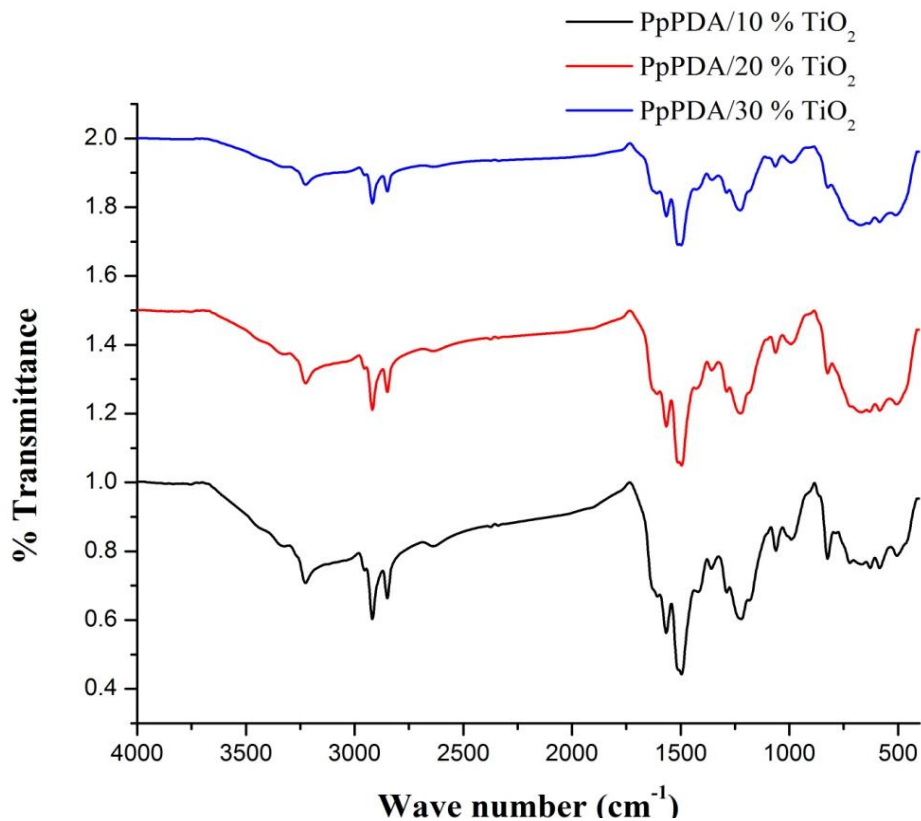
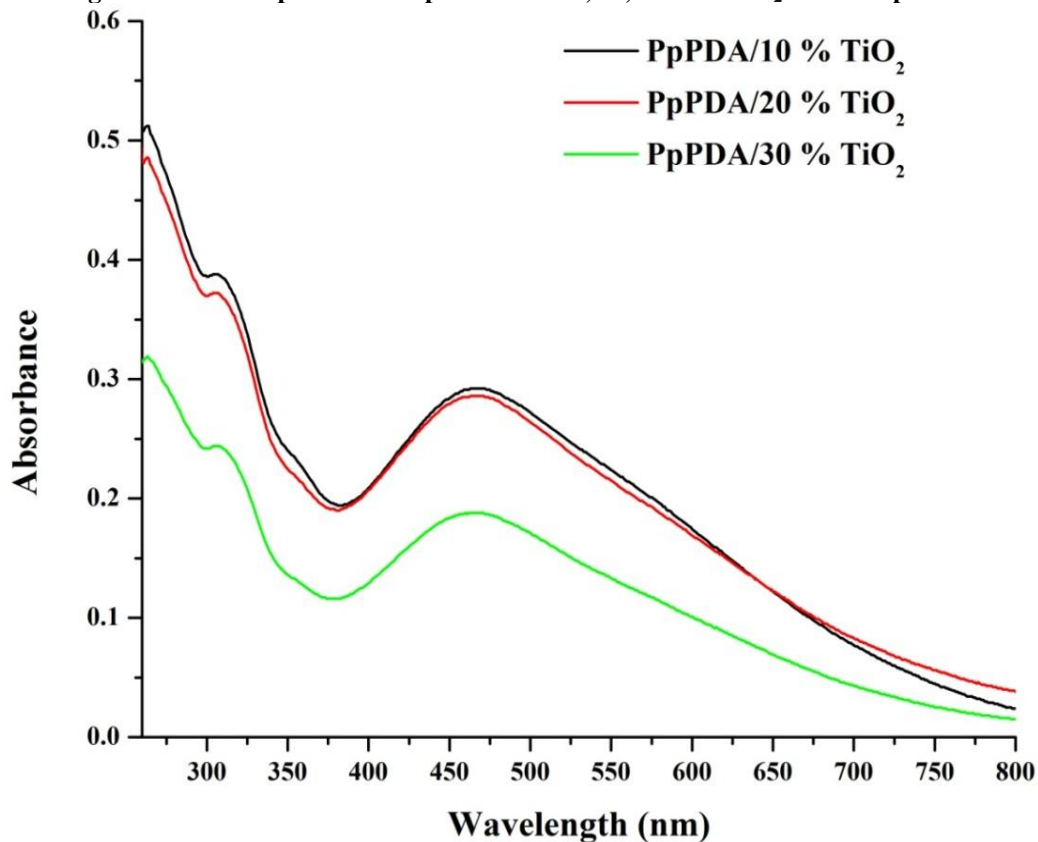
### 3.10 AC conductivity

The  $\sigma_{ac}$  conductivity of PpPDA/10%TiO<sub>2</sub>, PpPDA/20%TiO<sub>2</sub> and PpPDA/30%TiO<sub>2</sub> nanocomposites at room temperature at different frequencies are presented in Fig. 13. The conductivity of nanocomposites increases with increasing frequencies and obeys universal power law (Li Yu et al., 2012). The conductivity is almost constant up to 10<sup>4</sup> Hz and suddenly increases with increase in frequencies and this is the characteristic property of the disordered materials. Among all composites 30wt% shows high conductivity then the nanocomposites.

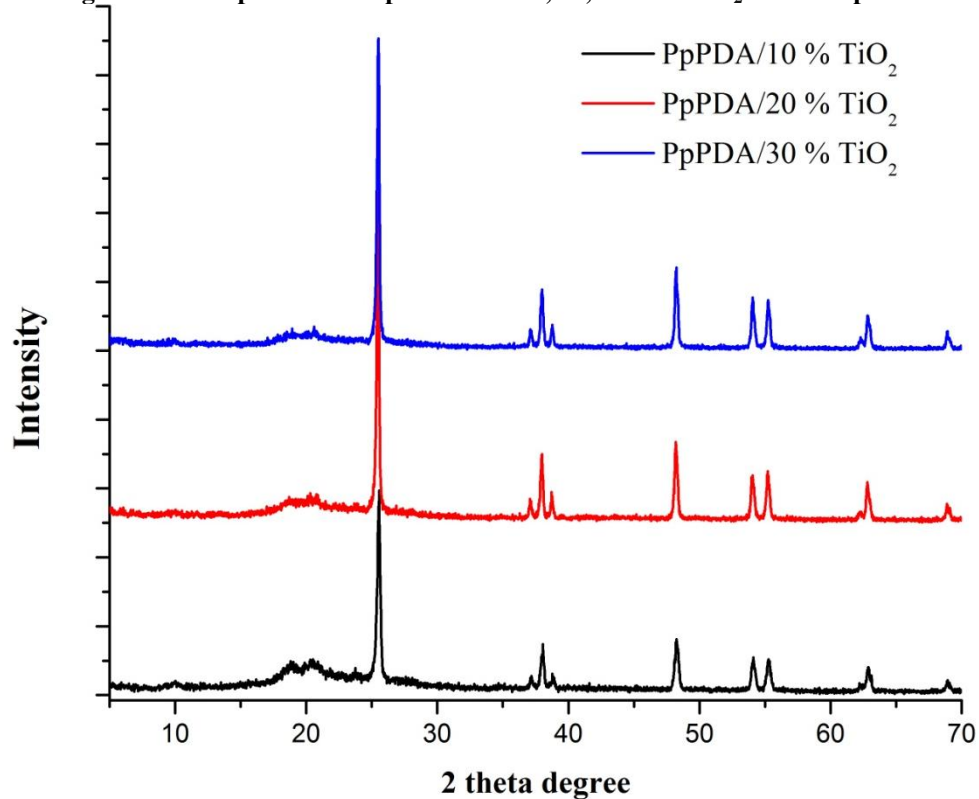
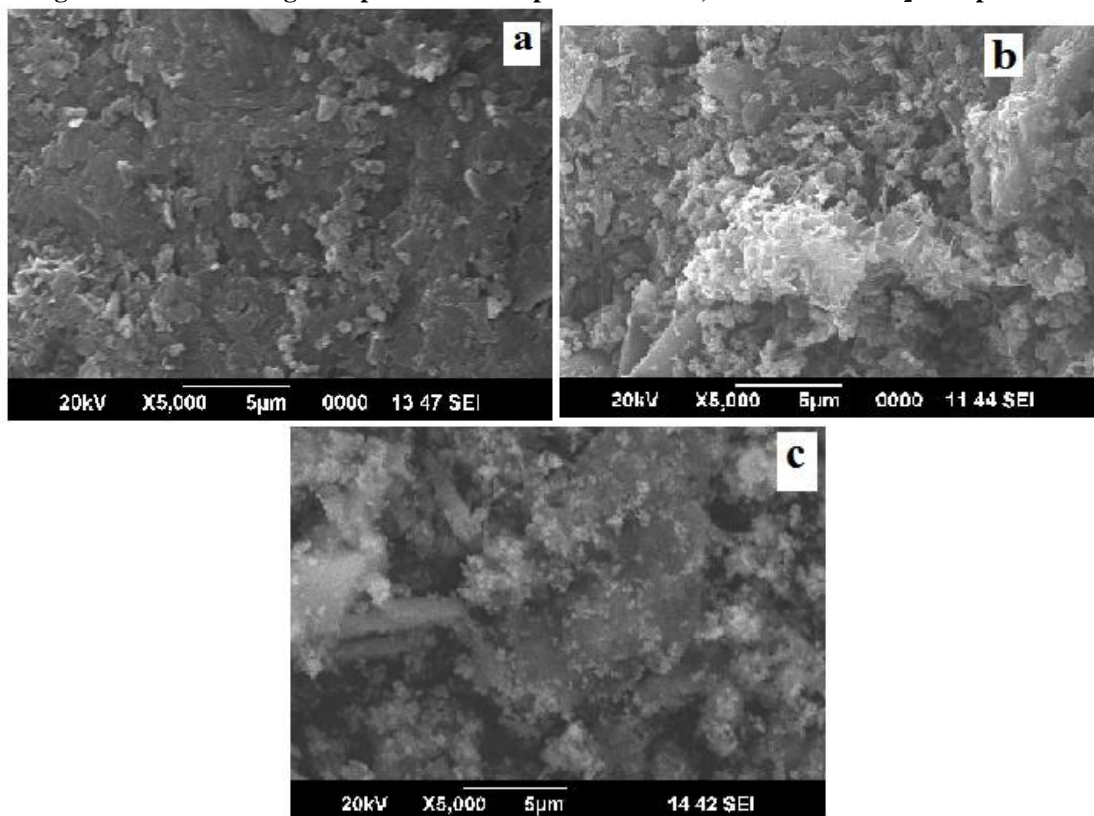
The complex impedance spectra measured at 30°C for 10, 20 and 30 wt. % of TiO<sub>2</sub>nanoparicles are shown in Fig.14. The conductivity values of PpPDA nanocomposites were evaluated using bulk resistance ( $R_b$ ) using the formula

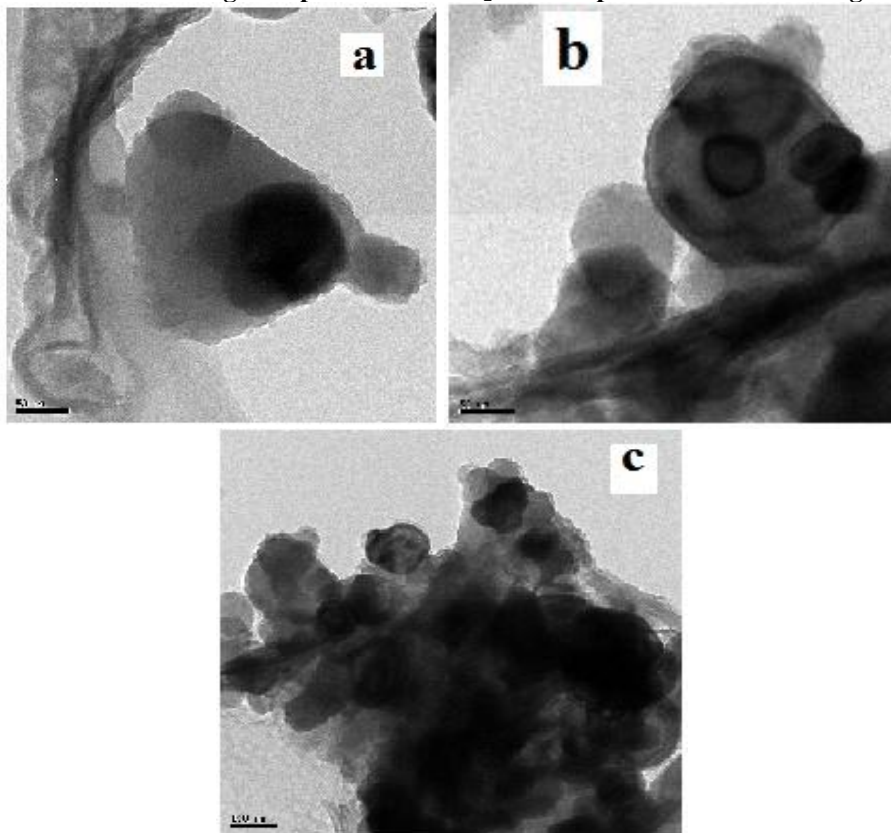
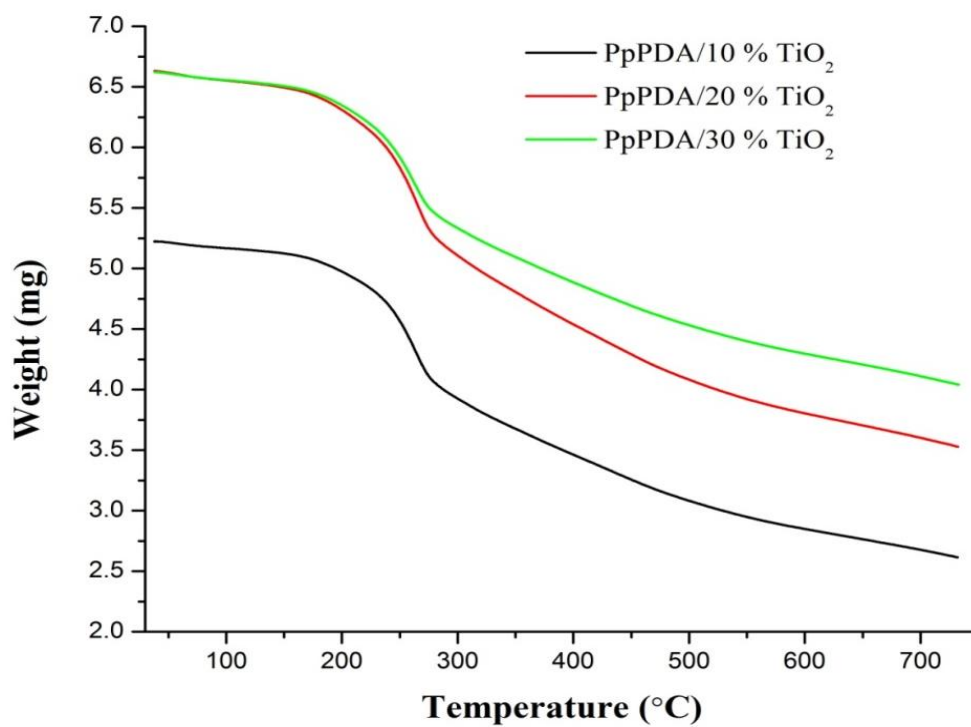
$$\sigma = (t / A) (1 / R_b) \text{ S/cm}$$

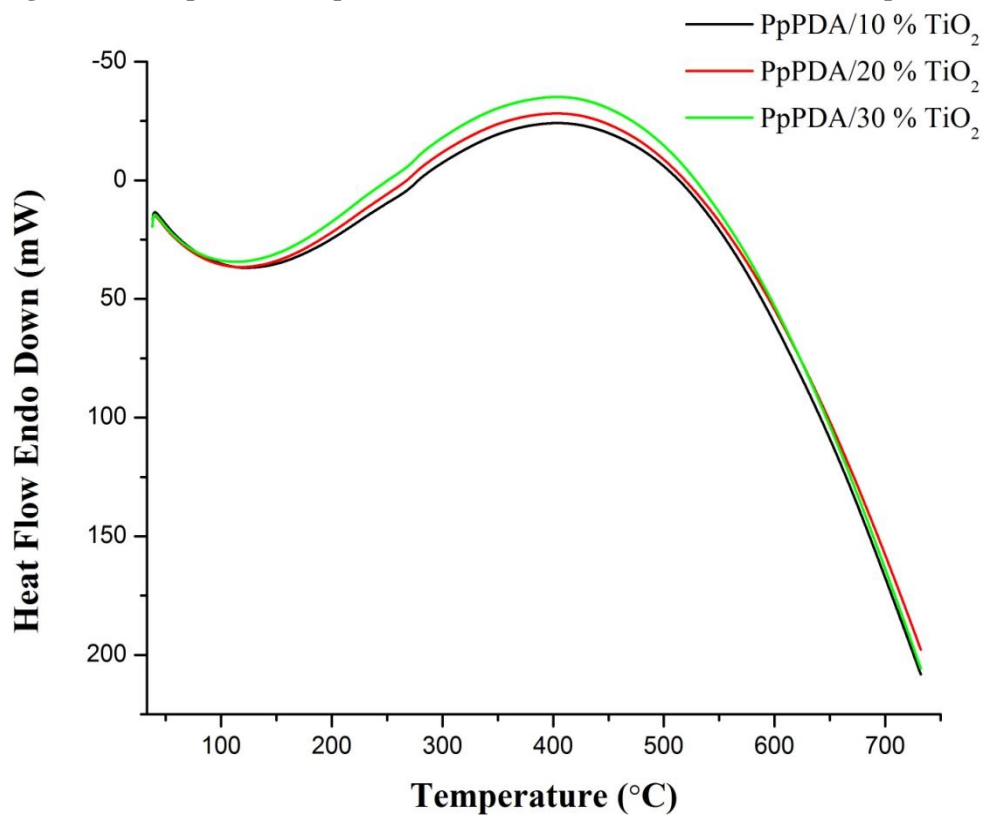
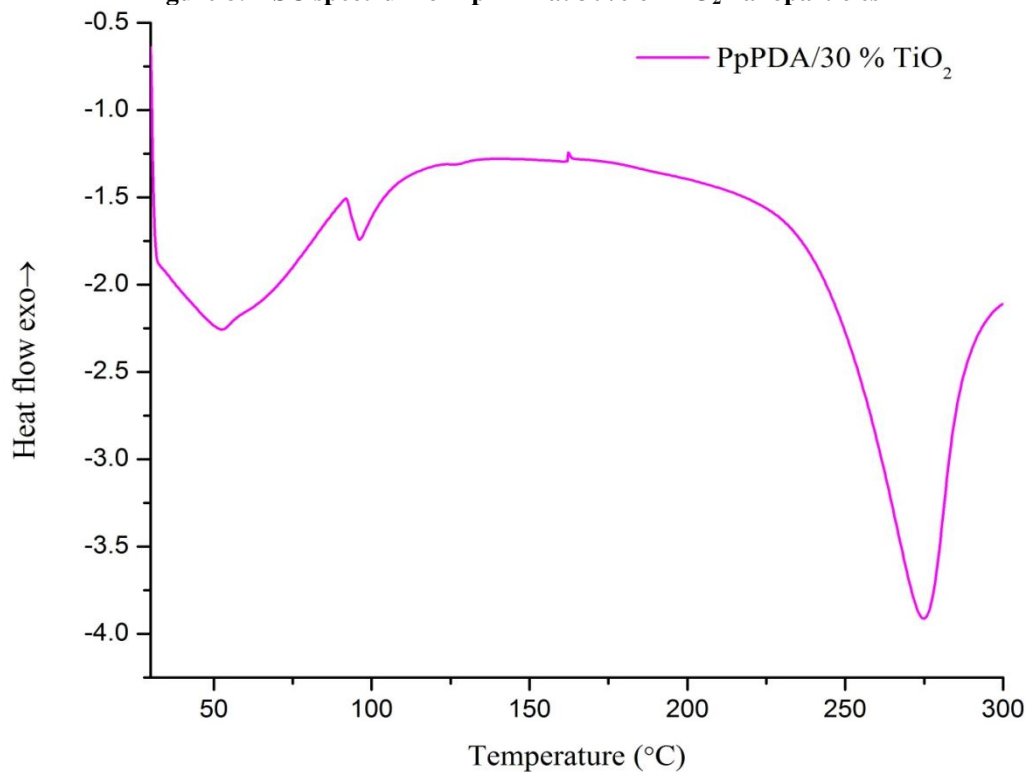
Where, t is the thickness of the pellet, A is the area of pellet, the sample film, and  $R_b$  is the bulk resistance of the pellet. The conductivity of the polymer increases with the addition of TiO<sub>2</sub> nanoparticles from 10<sup>-7</sup> into 10<sup>-5</sup> (Padmaraj et al., 2013). The AC conductivity of the PpPDA synthesized with 10, 20 and 30 % TiO<sub>2</sub> nanoparticles are found to be 1.4271 x10<sup>-5</sup>S/cm, 1.8047 x10<sup>-5</sup> S/cm and 2.1326 x10<sup>-5</sup> S/cm respectively. The difference in concentration of TiO<sub>2</sub> did not play any vital role in increasing the conductivity.

**Figure1: FT-IR spectrum of PpPDA with 10, 20, 30% of TiO<sub>2</sub> nanocomposites****Figure 2: UV-Vis spectrum of PpPDA with 10, 20, 30% of TiO<sub>2</sub> nanocomposites**

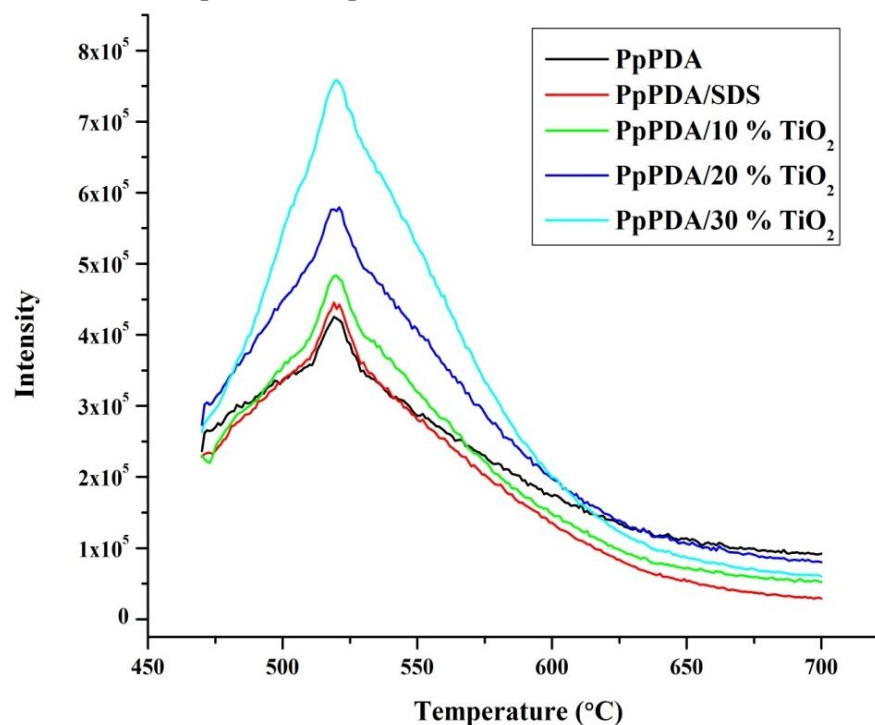
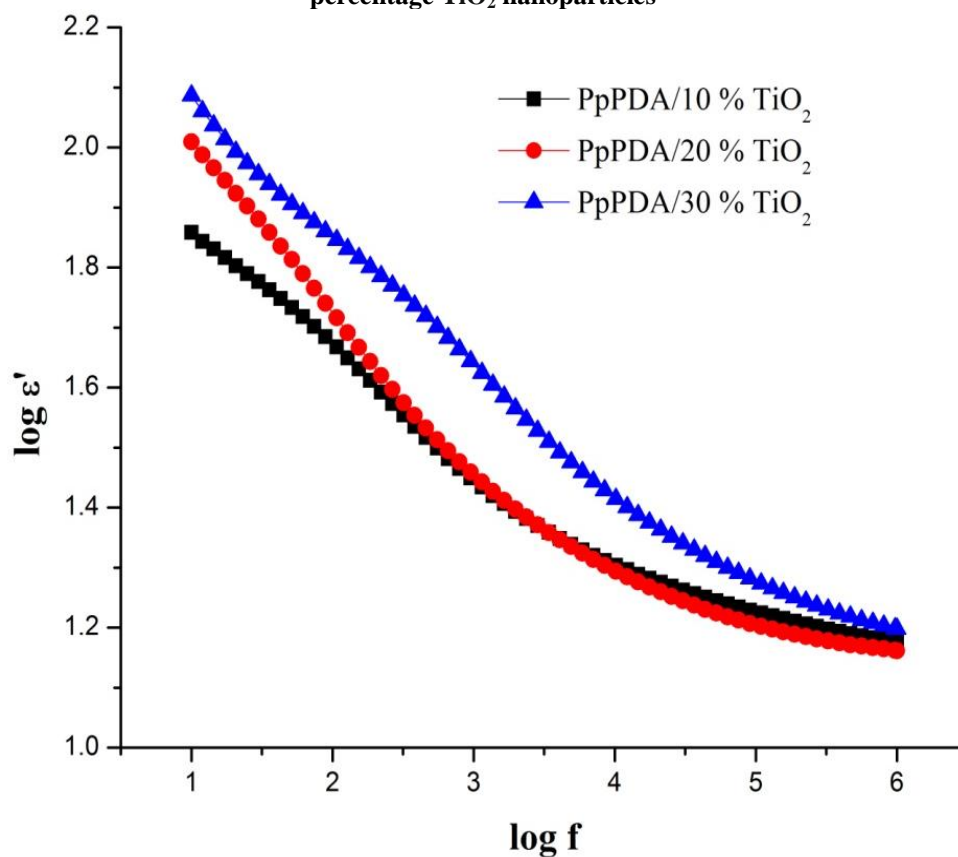


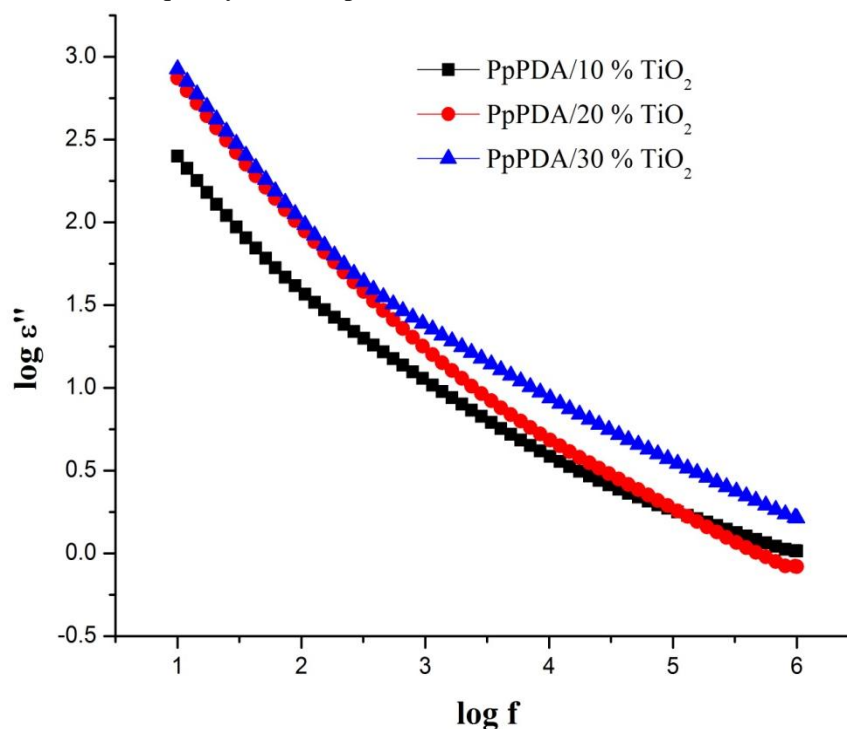
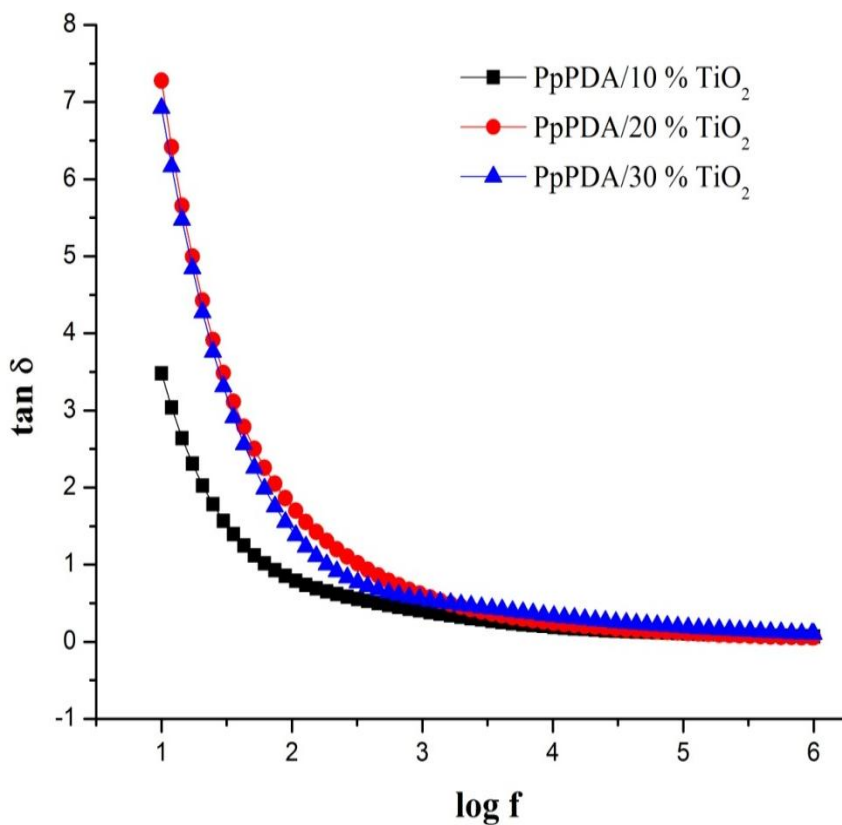
**Figure3: XRD spectrum of PpPDA with 10, 20, 30% of TiO<sub>2</sub> nanocomposites****Figure 4a-c: SEM image of PpPDAnanocomposites with 10, 20 and 30% TiO<sub>2</sub> nanoparticles**

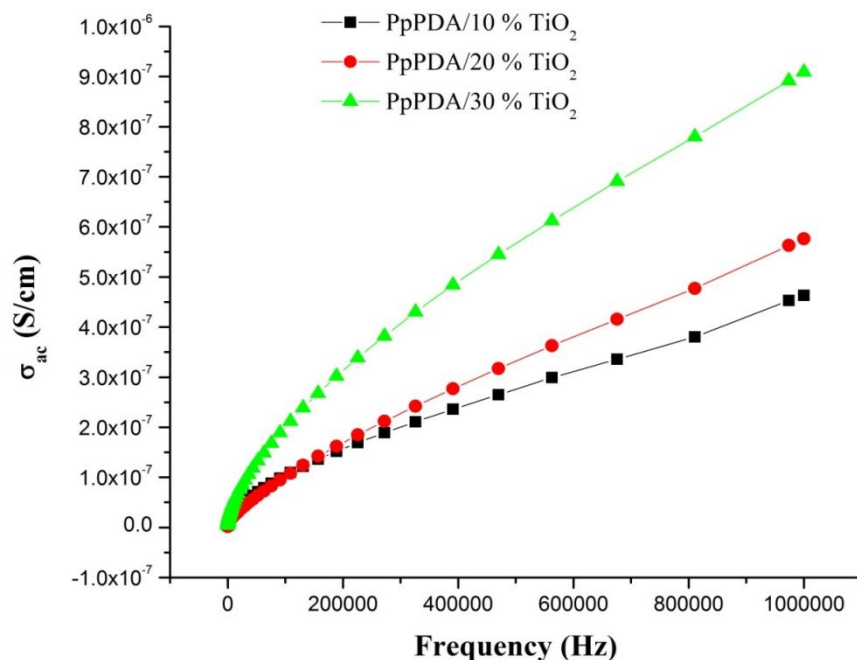
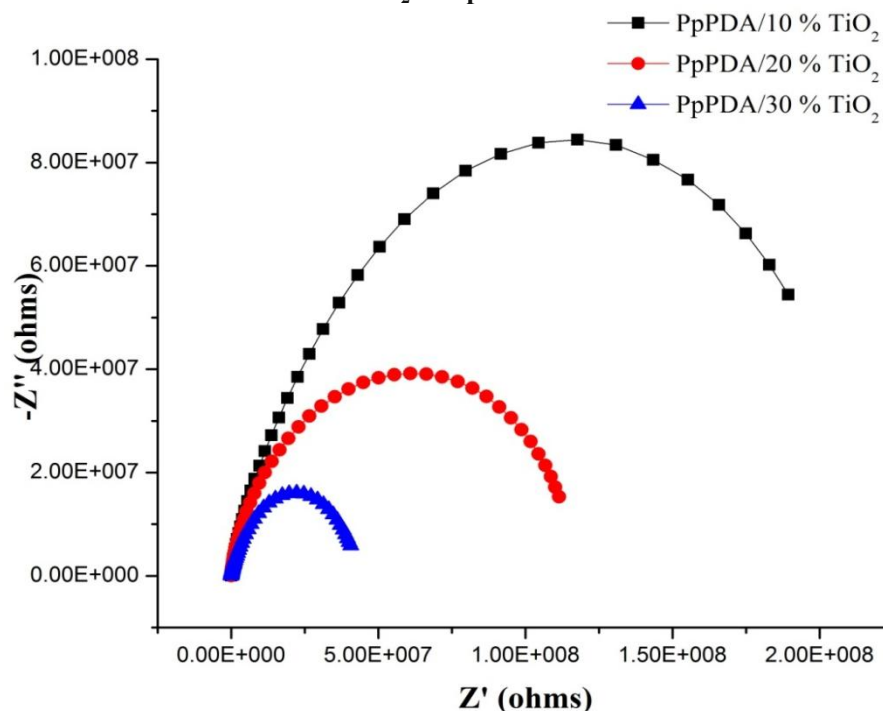
**Figure 5a-c: HRTEM image of PpPDA/30% TiO<sub>2</sub>nanocomposites at different magnification****Figure 6: TGA spectrum of PpPDA with different concentration of TiO<sub>2</sub> nanoparticles**

**Figure 7: DTA spectrum of PpPDA with different concentration of TiO<sub>2</sub> nanoparticles****Figure 8: DSC spectrum of PpPDA at 30% of TiO<sub>2</sub> nanoparticles**



**Figure 9: Photoluminescence spectrum of PpPDA with different concentrations of TiO<sub>2</sub>nanocompounds****Figure10: The plot  $\epsilon'$  against frequency for the PpPDAnanocomposites prepared with 10, 20, 30 weight percentage TiO<sub>2</sub> nanoparticles**

**Figure 11: Plots of  $\epsilon''$  Vs frequency for the PpPDA with different concentrations of  $\text{TiO}_2$  nanoparticles****Figure 12: Plots of  $\tan \delta$  Vs frequency for the PpPDA with different concentrations of  $\text{TiO}_2$  nanoparticles**

**Figure13: Plots of  $\sigma_{ac}$  Vs frequency of PpPDA with different concentrations of  $TiO_2$  nanoparticles****Figure 14: The complex impedance spectra of PpPDAnanocomposites prepared with different concentrations of  $TiO_2$ nanoparticles.**

## 5. Conclusion

The  $TiO_2$  nanocomposites of PpPDA have been successively prepared via chemical oxidative polymerization method. The synthesized polymer nanocomposites were characterized using FT-IR, UV-Vis spectroscopy and from the result it is confirmed the formation of the polymers. The morphology was studied by XRD, SEM and TEM and confirmed that the synthesized nanocomposites were of highly crystalline in nature and the formation of core shell type morphology of  $TiO_2$  nanoparticles incorporated into the polymer shell were confirmed. From the thermal analysis like TG/DTA, DSC, the polymer stability were analyzed and found to be thermally more stable. The PpPDA / $TiO_2$  nanocomposites have increased in electrical conductivity when compare to

the PpPDA. Dielectric analysis of the polymer and their nanocomposites shows that these materials can be used as energy storage devices, semiconductor devices, piezoelectric transducers, dielectric amplifiers etc.

## References

1. Aashish Roy; Ameena Parveen; Raghunandan Deshpande; Ravishankar Bhat; Anilkumar Koppalkar, (2013): Microscopic and dielectric studies of ZnO nanoparticles loaded in ortho-chloropolyaniline nanocomposites, *Journal of Nanoparticle Research*, 15: 1-11.
2. Alan Riga, Ricardo Collins, Gregory Mlachak, (1998): Oxidative behavior of polymers by thermogravimetric analysis, differential thermal analysis and pressure differential scanning calorimetry, *Thermochimica Acta*, 324: 135-149.
3. Bluma G. Soares, Maria Elena Leyva, Guilherme M.O. Barra, Dipak Khastgir, (2006): Dielectric behavior of polyaniline synthesized by different techniques, *European Polymer Journal*, 42: 676-686.
4. Deivanayaki, S., Ponnuswamy, V., Mariappan, R., Jayamurugan, P., (2012): Synthesis and characterization of polypyrrole/TiO<sub>2</sub> composites by chemical oxidative method, *Optik*, 124: 1089-1091.
5. Elsayed A.H., Mohy Eldin M. S., Elsyed A.M., Abo Elazma H., Younes E.M., and Motaweh, H. A., (2011): Synthesis and Properties of Polyaniline/ferrites Nanocomposites, *International Journal of Electrochemical Science*, 6: 206 - 221.
6. Hui-Long Wang, De-Ying Zhao, Wen-Feng Jiang, (2012): Synthesis and photocatalytic activity of poly(o-phenylenediamine (PoPD)/TiO<sub>2</sub> composite under VIS-light irradiation, *Synthetic Metals*, 162: 296-302.
7. Jalal Arjomandi; Sahar Tadayyonfar, (2014): Electrochemical Synthesis and In Situ Spectroelectrochemistry of Conducting Polymer Nanocomposites. I. Polyaniline/TiO<sub>2</sub>, Polyaniline/ZnO, and Polyaniline/TiO<sub>2</sub>+ZnO, *Polymer composites*, 35: 351-363.
8. Liang Wang, Shaojun Guo, Shaojun Dong, (2008): Facile synthesis of poly(o-phenylenediamine) microfibrils using cupric sulfate as the oxidant, *Materials Letters*, 62: 3240-3242.
9. Li Yu, Yihe Zhang, Wangshu Tong, Jiwu Shang, Fengzhu Lv, Paul K. Chu and Wenmin Guo, (2012): Hierarchical composites of conductivity controllable polyaniline layers on the exfoliated graphite for dielectric application, *Composites: Part A*, 43: 2039-2045.
10. Machappa, T.; and Ambika Prasad, M.V.N., (2009) AC conductivity and dielectric behavior of polyaniline/sodium metavanadate (PANI/NaVO<sub>3</sub>) composites, *Physica B*, 404: 4168-4172.
11. Matthew J. Thompson; David C. Whalley and Neil Hopkinson, (2008): Investigating dielectric properties of sintered polymers for rapid manufacturing, 79-93.
12. Meirong Wang, Huaihao Zhang, Chengyin Wang, Guoxiu Wang, (2013): Synthesis of MnO<sub>2</sub>/poly(o-phenylenediamine) composite and its application in supercapacitors, *Electrochimica Acta*, 106: 301-306.
13. Mei-Rong Huang; Xin-Gui Li; Yuliang Yang, (2001): Oxidative polymerization of o-phenylenediamine and pyrimidylamine, *Polymer Degradation and Stability*, 71: 31-38.
14. Mona H. Abdel Rehim; Nahla Ismail, Abd El-Rahman A.A. Badawy, Gamal Turkey, (2011): Poly phenylenediamine and its TiO<sub>2</sub> composite as hydrogen storage material, *Materials Chemistry and Physics*, 128: 507-513.
15. Muthirulan, P., Kannan, N., Meenakshisundaram, M., (2013): Synthesis and corrosion protection properties of poly(o-phenylenediamine) nanofibers, *Journal of Advanced Research*, 4: 385-392.
16. Muthirulan. P., and Rajendran N., (2012): Poly (o-phenylenediamine) coatings on mild steel: Electrosynthesis, characterization and its corrosion protection ability in acid medium, *Surface & Coatings Technology*, 206: 2072-2078.
17. Padmaraj, O., Venkateswarlu, M., and Satyanarayana, N., (2013): Effect of ZnO filler concentration on the conductivity, structure and morphology of PVdF-HFP nanocomposite solid polymer electrolyte for lithium battery application, *Ionics*.
18. Pandi Muthirulan, Chenthamarai Kannan Nirmala Devi, Mariappan Meenakshi Sundaram, (2013): Facile synthesis of novel hierarchical TiO<sub>2</sub>@Poly(o-phenylenediamine) core shell structures with enhanced photocatalytic performance under solar light, *Journal of Environmental Chemical Engineering*, 1: 620-627.
19. Paulo Meneghetti, Syed Qutubuddin, (2006): Synthesis, thermal properties and applications of polymer-clay nanocomposites, *Thermochimica Acta*, 442: 74-77.
20. Paulraj, P., Janaki, N., Sandhya, S., Pandian, K., (2011): Single pot synthesis of polyaniline protected silver nanoparticles by interfacial polymerization and study its application on electrochemical oxidation of hydrazine, *Colloids and Surfaces A: Physicochem. Eng. Aspects*, 377: 28-34.
21. Pengwei Huo, Yongsheng Yan, Songtian Li, Huaming Li, Weihong Huang, (2010): Preparation of poly(o-phenylenediamine)/TiO<sub>2</sub>/fly-ash cenospheres and its photo-degradation property on antibiotics, *Applied Surface Science*, 256: 3380-3385.

22. PerkinElmer; United Kingdom, An introduction to fluorescence spectroscopy, **2000**.
23. Rajeev sehwat, (2009) Synthesis and characterization of PANI-ZnO composite, Tharpar University.
24. Ramesh Patil, Aashis S. Roy, Koppalkar R. Anilkumar, Jadhav, K.M, ShrikantEkhelkar, (2012): Dielectric relaxation and ac conductivity of polyaniline–zinc ferrite composite, Composites: Part B,43: 3406–3411.
25. Siwei Yang, Dong Liu, Fang Liao, TingtingGuo, Zhiping Wu, Tingting Zhang, (2012): Synthesis, characterization, morphology control of poly (p-phenylenediamine)-Fe<sub>3</sub>O<sub>4</sub> magnetic micro-composite and their application for the removal of Cr<sub>2</sub>O<sub>7</sub><sup>2-</sup> from water, Synthetic Metals, 162: 2329– 2336.
26. SubodhSrivastava, Sumit Kumar, Singh, V. N., Singh, M., and Vijay, Y.K., (2011): Synthesis and characterization of TiO<sub>2</sub> doped polyaniline composites for hydrogen gas sensing, International Journal of Hydrogen Energy, 36:6343-6355.
27. Xiaofeng Lu, Hui Mao, Danming Chao, Xiaogang Zhao, Wanjin Zhang and Yen Wei, (2007): Preparation and characterization of poly(o-phenylenediamine) microrods using ferric chloride as an oxidant, Materials Letters, 61:1400–1403.